Virus Research 274 (2019) 197773

Contents lists available at ScienceDirect

Virus Research

journal homepage: www.elsevier.com/locate/virusres

Bioinformatically-predicted varicella zoster virus small non-coding RNAs are expressed in lytically-infected epithelial cells and neurons

Linoy Golani-Zaidie[a,1], Tatiana Borodianskiy-Shteinberg[a,1], Punam Bisht[a], Biswajit Das[a], Paul R. Kinchington[b], Ronald S. Goldstein[a,*]

[a] Mina and Everard Goodman Faculty of Life Sciences Bar-Ilan University, Ramat-Gan, 5900002, Israel
[b] Departments of Ophthalmology and of Microbiology and Molecular Genetics, University of Pittsburgh, 1020 EEI 203 Lothrop Street, Pittsburgh PA 15213-2588, United States

ARTICLE INFO

Keywords:
Non-coding RNA
Varicella zoster virus
Human neurons
Neurotropic virus

ABSTRACT

Most herpesviruses use both host and viral small non-coding RNAs (sncRNA), especially microRNA, to modulate infection. Bioinformatic analyses of NGS data obtained from Varicella Zoster virus (VZV)-infected cells predicted 24 VZVsncRNA, seven of which were confirmed to be expressed in infected fibroblasts and neurons using stem-loop quantitative reverse transcription PCR (SL-PCR). We here assayed for the expression of all 24 of the bioinformatically predicted VZVsncRNA in cells productively infected by VZV using SL-PCR. 23 of the 24 predicted sequences were detected in VZV-infected ARPE19 cells and 19 of the 24 sequences in infected human neurons generated by two methods from embryonic stem cells. We also show that blocking one of two newly-tested VZV-encoded sncRNA using locked nucleotide antagonists significantly increased viral replication. These findings suggest that further study of VZV encoded sncRNA could elucidate an additional level of regulation of the life cycle of this pathogenic human herpesvirus.

1. Introduction

A recent focus of the herpesvirus field has been non-coding and microRNAs and how they may control viral growth, latency and reactivation (reviewed in (Cullen, 2011; Piedade and Azevedo-Pereira, 2016). Varicella Zoster virus (VZV, human herpesvirus-3) is a pathogenic neurotropic human alphaherpesvirus, causing varicella (chickenpox) upon primary infection and herpes zoster (shingles) upon reactivation from latency in the peripheral nervous system. The study of how VZV growth might be regulated by non-coding RNAs has lagged behind that of other human herpesviruses. Two published NGS studies of latently infected human post-mortem ganglia failed to reveal any sequences with the characteristics of miRNAs encoded by VZV (Umbach et al., 2009; Depledge et al., 2018). However, a recent study of the VZV transcriptome using long-read NGS has detected dozens of non-coding RNAs (Prazsák et al., 2018). In addition, a recent study of enriched viral RNA from human ganglia has suggested that latency is associated with multiple spliced transcripts that could encode small non-coding RNAs (Depledge et al., 2018).

We recently reported that NGS analyses of small (< 200 nucleotides, nt) RNA in lytically-infected cultured human fibroblasts and neurons revealed at least 24 sequences of 22–24 nt encoded by VZV, one of which was predicted to fold into a miR structure (Markus et al., 2017). The sequences of these potential small non-coding RNAs were predicted based on a novel bioinformatic analysis using manual alignment of similar sequences from multiple reads. That study confirmed the presence of 7 of these putative VZVsncRNA using stem-loop quantitative reverse-transcriptase-PCR (SL-PCR) in VZV infected human fibroblasts. NGS counts representing all the predicted VZVsncRNA were also detected in small RNA extracted from human embryonic stem cell (hESC) derived neurons infected productively with VZV, although presence of only one was confirmed by SL-PCR. hESC-derived neurons latently-infected with VZV also yielded NGS reads for several of the VZVsncRNA. Given the current interest in the roles of multiple types of viral non-coding RNA in gene control of expression of the herpesvirus life-cycle, it is important to further investigate which of the NGS reads

Abbreviations: BDNF, brain derived neurotrophic factor; sncRNA, small non-coding ribonucleic acids; dpi, days post infection; GFP, green fluorescent protein; FOI, focus of infection; GDNF, glia-derived neurotrophic factor; hESC, human embryonic stem cell; LNA, locked nucleic acid; NGS, next generation sequencing; NGF, nerve growth factor; NT3, neurotrophic factor 3; SL-PCR, stem-loop polymerase chain reaction; VZV, varicella zoster virus

* Corresponding author at: Mina and Everard Goodman Faculty of Life Sciences, Gonda Building, Old Campus, 5290002 Ramat-Gan, Israel.
E-mail address: ron.goldstein@biu.ac.il (R.S. Goldstein).

[1] Equal contribution.

https://doi.org/10.1016/j.virusres.2019.197773
Received 2 August 2019; Received in revised form 10 September 2019; Accepted 4 October 2019
Available online 12 October 2019
0168-1702/

of small RNAs could be detected in VZV-infected cells using an independent assay.

We report here the results of a survey for the VZVsncRNA using Taqman SL-PCR for all of the 24 VZVsncRNA we predicted to be encoded by the virus in samples of small RNA (< 200 nt) extracted from productively infected ARPE19 cells, which are highly permissive for VZV replication, and from productively infected human neurons derived from human embryonic stem cells (hESC, (Pomp et al., 2005), (Birenboim et al., 2013)). In order to investigate whether expression of VZV-encoded sncRNA may contribute to the regulation of VZV replication, we measured infectious focus growth (Markus et al., 2017) and performed plaque assays with VZV-infected ARPE19 cells transfected with specific locked-RNA antagonists to two of these VZVsncRNA.

2. Materials and methods

2.1. Viruses, infection and cells

The VZV used in these studies were a recombinant virus expressing GFP as an N terminal fusion to ORF66 (VZV66GFP), derived from parent of Oka cosmids as detailed previously (Erazo et al., 2008) and a similar virus expressing monomeric red fluorescent protein (mRFP) linked to the N terminus of ORF66, VZV66RFP, made by recombineering of a self-excisable VZV BAC originally described in (Tischer et al., 2007) and generated as detailed previously (Markus et al., 2017). Infection of ARPE19 cells (ATCC) and neurons was performed using cell-associated or cell-free virus obtained from sonicates of infected cells, either as the low speed supernatant or the pelleted debris fraction, as detailed previously (Sloutskin and Goldstein, 2014). Cells were harvested when at least 60% of cells were fluorescent, typically 4–5 days for ARPE cells and 6–7 days for neuronal cultures.

The human embryonic stem cell (hESC) line H9 (WA09) was maintained on STO feeder cells in Nutristem (Biological Industries, Israel) medium and differentiated to neurons using two methods. The first method used PA6 stromal cell induction (Kawasaki et al., 2000) as described in detail (Pomp et al., 2005). The second method was a modification of the method in Birenboim et al using agarose microwells (Birenboim et al., 2013). Briefly, hESC were dissociated with Accutase (Sigma-Aldrich), and 750,000 cells seeded into a 256-well agarose microwell dish made using silicone molds (Sigma-Aldrich). The cells were aggregated for 4 days in the molds in a medium consisting of: GMEM (Gibco/Life Technologies) 1% penicillin/ streptomycin (Biological Industries (BI), 1% L-glutamate (BI) 1% pyruvate (BI), 10% KSR – knockout serum replacement (Gibco), 1% non-essential amino acids (BI), 0.1μm mercaptoethanol (Sigma-Aldrich), with BMP4 inhibitors SB431542 (10μm) and dorsomorphin (2μm) (Tocris Bioscience). The aggregates were then grown for an additional 10 days in the same medium lacking the inhibitors. This was followed by plating the aggregates on polylysine/laminin (Sigma-Aldrich) coated coverslips or tissue culture plates in differentiation medium consisting of DMEM/F12 with neural growth and survival factors NGF, BDNF, NT3 and GDNF (Alomone Labs) and B27 supplement. Dividing cells were eliminated from the cultures using the mitotic inhibitors 24μM 5-fluorodeoxyuridine (F0503, Sigma-Aldrich) and 0.6μM cytosine arabinoside (C6645, Sigma-Aldrich) added 4 days after plating. 24μM Uridine (U3750, Sigma-Aldrich) was added to the medium in order to offset the toxicity of the fluordeoxyuridine. Neuronal cultures were maintained for a total of 10–14 days after removal from the molds. Immunofluorescent staining for neurofilament proteins was performed with antibody 2H3 to the intermediate neurofilament subunit (NF-M) deposited to the Developmental Studies Hybridoma Bank by Jessell, T.M. and Dodd, J., and Sigma-Aldrich (Merck) N4142 to the heavy neurofilament subunit (NF-H).

2.2. RNA preparation and stem-loop Taqman PCR for sncRNA

RNA was extracted using the Hybrid-R kit for large RNA/small RNA (Geneall, South Korea). RNA was treated with DNase (AMPD1, Sigma-Aldrich). All primers and probes were designed as described in (Mohammadi-Yeganeh et al., 2013). Primers were generated by Sigma-Aldrich (Israel) and the probe was LGC Biosearch Technologies DLO-RFB-5 (California, USA). The cDNA for each sncRNA was prepared in separate reactions and converted to cDNA using MMLV reverse transcriptase (Promega, # M1701) at increasing temperatures: 25 °C for 15 min, 37 °C for 15 min, 42 °C for 40 min and finally 95 °C for enzyme inactivation. qPCR reactions were performed with qPCRBIO probe mix Hi-ROX (PCR Biosystems) using universal reverse and specific forward primers. All qPCR reactions were performed in triplicate and averaged to compensate for pipetting errors.

2.3. Transfection of synthetic antagonists to VZV sncRNA and measurement of their effect on VZV replication

Details of these procedures were described in our previous study (Markus et al., 2017). In brief, monolayers of ARPE19 cells at approximately 80% confluence were infected with VZV66RFP-infected ARPE19 cells at several concentrations in 96 well black-walled tissue culture plates. Wells chosen for analysis had approximately 10–30 infected cells 1dpi that would develop into well-separated infectious foci (FOI) whose growth could be followed individually. At 1dpi, triplicate wells were transfected with a synthetic antagonist RNA to VZV sncRNA or scrambled RNA (Exiqon) using Dharmafect2 (Dharmacon) according to the manufacturer's instructions.

An automated microscope was then used to photograph entire wells daily (36 images/well) using Micromanager v1.4 (https://micromanager.org/wiki/)in both fluorescence and brightfield illumination. The micrographs were "stitched" together using the program Fiji and the resulting composite images covered more than 95% of each well. The composites generated in this manner were processed to enhance contrast for clearly identifying the FOI. The course of progression of growth of individual FOI was measured using ImageJ (https://imagej.nih.gov/ij/). Quantification of infectious virus was determined by plaque assays of cells collected on the last day of imaging (5-6dpi) and then seeded on naïve ARPE19 cells. After 5 days, cultures were fixed, stained with Crystal violet, and plaques counted. Data is represented as the average ± the standard error of the mean. T-tests using equal variance and two tails were performed with Microsoft Excel.

3. Results

3.1. VZV-infected ARPE19 cells express 23 of 24 bioinformatically-predicted VZVsncRNA

Stem-loop qPCR (SL-PCR) was performed on small (< 200 nt) RNA extracted from VZV66GFP-infected ARPE19 cells (Fig. 1A–C) using specific primers (Table 1) designed for all 24 previously predicted VZVsncRNA (Markus et al., 2017). Evaluation of NGS results for human sncRNA showed that the expression of hsa-mir26 was at a high level and showed little variation from sample to sample (Markus et al., 2017) therefore SL-PCR was performed for this sncRNA in each sample and used to normalize the expression of the VZVsncRNA (Watson et al., 2007).

We obtained small RNA fractions from VZV-infected ARPE19 cells from 8 independent experiments. Amplification of 23 of the 24 VZVsncRNA sequences was detected at a difference of at least 3 PCR cycles in at least one infection/extraction of RNA, and most sncRNA sequences were detected in the majority of at least 3 independent infections/RNA extractions (Table 2). VZVsncRNA15, VZVsncRNA20, VZVsncRNA21 and VZVsncRNA22 were amplified in only one of 3, 5, 2 and 7 experiments respectively. Because of the limited amounts of RNA

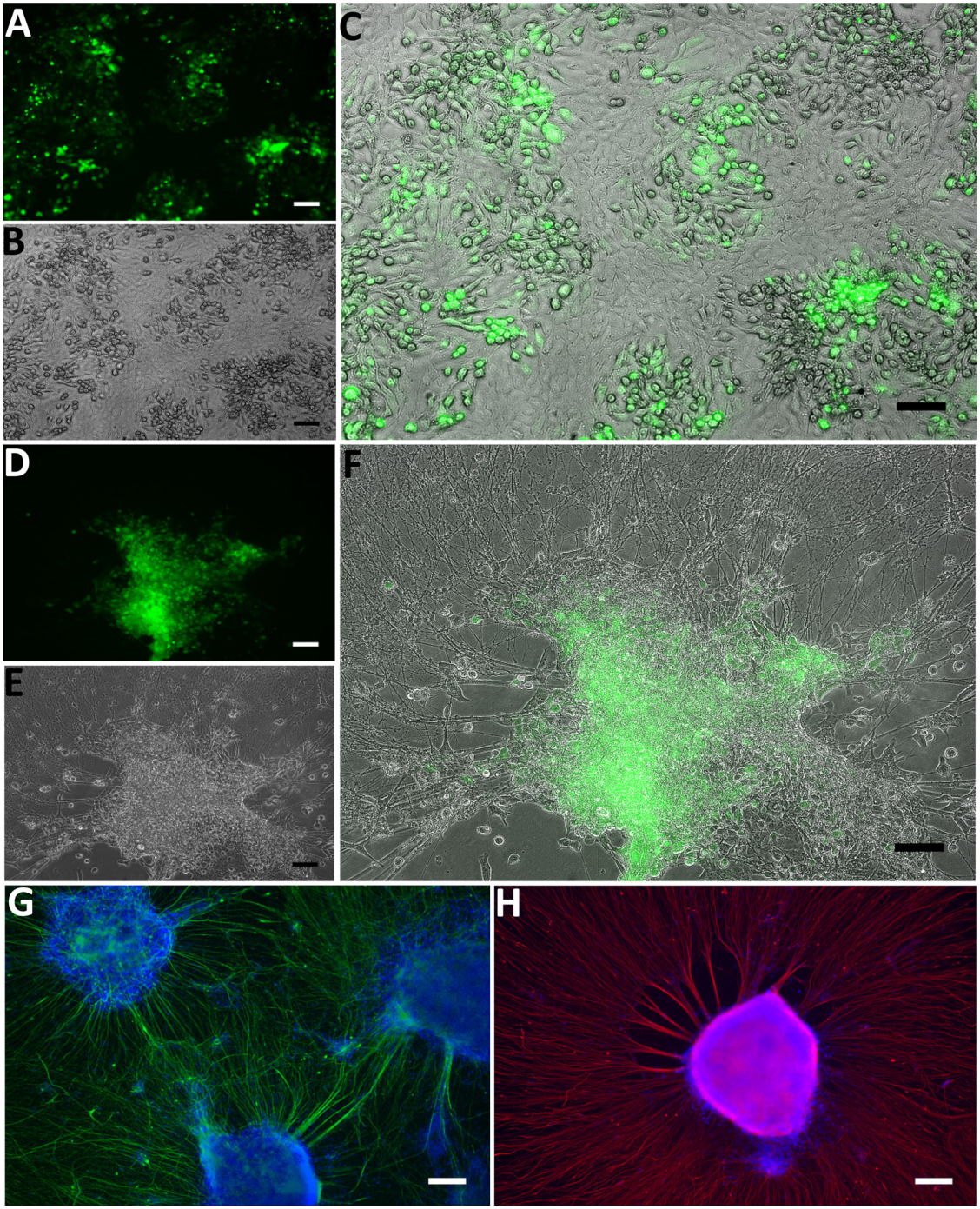

Fig. 1. Micrographs of VZV-infected cultures and immunostained human neurons.
(A–C) A living culture of ARPE19 cells infected in a cell-associated manner with VZVGFP66 at 4dpi Panel A = GFP fluorescence reporting ORF66 protein expression; panel B, phase contrast and panel C, a merged image of A and B. (D–F) A living culture of human neurons derived without feeder cells that were infected in a cell-associated manner with VZVGFP66 at 6 dpi. Panel D shows GFP fluorescence; panel E shows phase contrast; panel F shows a merge of the images in D and E. Panels G and H show fixed cultures of uninfected neurons immunostained for neurofilament medium (G- green) and heavy (H-red) subunits. Nuclei are stained with Hoeschst (blue). Bars depict 100μm in all panels.

obtained from the small-RNA isolation kit and variable efficiency of extraction, we only assayed for some of the VZVsncRNA in each experimental infection/extraction. The quantitative results from two experiments are shown in Supplementary Table 1. As can be seen in the Supplementary table, the VZVsncRNA were detected at very different levels, both within and between experiments (see discussion).

The only bioinformatically predicted VZVsncRNA we did not detect by SL-PCR in VZV infected ARPE19 was VZVsncRNA3, which was not amplified in four separate preparations of RNA from independent infections. We note that the frequency of detection of VZVscnRNA detected with SL-PCR did not correlate with the number of NGS reads reported previously in infected fibroblasts. An extreme example was VZVsncRNA22, whose sequences were present at the second highest levels in infected fibroblasts in our NGS study (Markus et al., 2017) but was detected in only one of 7 RNA preparations of VZV-infected ARPE19 cells.

Table 1
Primers and probes used in this study.

sncRNA	sequence	start	end	ORF	Stem-loop primer	Fwd. primer
VZVsncRNA1	CCCCTTCCGGACAGTAGTTTC	561	581	ORF0	GGTCGTATGCAAGAGCAGGGTCCGAGGTATCCATCGCACGCATCGCACTGCATACGACCGAAACTAC	TATAGTACCCCTTCCGGACA
VZVsncRNA2	TACCGTAGAACTACGCGCCCGGGA	12642	12665	ORF10	GGTCGTATGCAAGAGCAGGGTCCGAGGTATCCATCGCACGCATCGCACTGCATACGACCTCCCGGGC	GACTGATACCGTAGAACTACGC
VZVsncRNA3	TCTGAATAAAATGTTTAGC	30918	30936	ORF21	GGTCGTATGCAAGAGCAGGGTCCGAGGTATCCATCGCACGCATCGCACTGCATACGACCGCTAAACA	CCGCGGGCTCTGAATAAAA
VZVsncRNA4	CCGTGCATGTCTGGATTGAAGGG	68366	68388	ORF37	GGTCGTATGCAAGAGCAGGGTCCGAGGTATCCATCGCACGCATCGCACTGCATACGACCCCCTTCAA	TTAATTCCGTGCATGTCTGGA
VZVsncRNA5	TTGTTGCACCGGGGGACGTAGACC	73236	73259	ORF40	GGTCGTATGCAAGAGCAGGGTCCGAGGTATCCATCGCACGCATCGCACTGCATACGACCGGTCTACG	TATATTTGTTGCACCGGGGGA
VZVsncRNA6	CGCTAGACTGTTTTTCTGCTCA	80339	80360	ORF42	GGTCGTATGCAAGAGCAGGGTCCGAGGTATCCATCGCACGCATCGCACTGCATACGACCTGAGCAGA	GGCGCGCTAGACTGTTTT
VZVsncRNA7	ATGGCACGATCGGGATTGGATAG	84667	84689	ORF48	GGTCGTATGCAAGAGCAGGGTCCGAGGTATCCATCGCACGCATCGCACTGCATACGACCCTATCCAA	AATAATGGCACGATCGGGA
VZVsncRNA8	GAAATGTCGGTTTCTGCAGGGTG	85492	85514	ORF48	GGTCGTATGCAAGAGCAGGGTCCGAGGTATCCATCGCACGCATCGCACTGCATACGACCCACCCTGC	CGCGGAAATGTCGGTTTCT
VZVsncRNA9	ACCCGAGATCGATTGGAGTGTTAT	100306	100329	ORF59	GGTCGTATGCAAGAGCAGGGTCCGAGGTATCCATCGCACGCATCGCACTGCATACGACCATAACACT	ATGAGTACCCGAGATCGATTGG
VZVsncRNA10	TCAACCCGAAATTGTAGAGCCT	103664	103685	ORF61	GGTCGTATGCAAGAGCAGGGTCCGAGGTATCCATCGCACGCATCGCACTGCATACGACCAGGCTCTA	GCGCTATCAACCCGAAATTG
VZVsncRNA11	GAGACTCGAGCCCTGGTGTAACC	103976	103998	ORF61	GGTCGTATGCAAGAGCAGGGTCCGAGGTATCCATCGCACGCATCGCACTGCATACGACCGGTTACAC	TAAAGTATGAGACTCGAGCCCTG
VZVsncRNA12	GCCCGGACATTAGAATACAGCCAG	104494	104517	ORF61-5'UTR	GGTCGTATGCAAGAGCAGGGTCCGAGGTATCCATCGCACGCATCGCACTGCATACGACCCTGGCTGT	TAGAGGCCCGGACATTAGAAT
VZVsncRNA13	TTGGATGCCCGGACATTAGAATAC	104500	104523	ORF61-5'UTR	GGTCGTATGCAAGAGCAGGGTCCGAGGTATCCATCGCACGCATCGCACTGCATACGACCGTATTCTA	ATTTGGATGCCCGGACAT
VZVsncRNA14	CGCCCGGCGGTCAAGGTGGAGCT	105286	105308	ORF62	GGTCGTATGCAAGAGCAGGGTCCGAGGTATCCATCGCACGCATCGCACTGCATACGACCAGCTCCAC	AATCGCCCGGCGGTCAAG
VZVsncRNA15	CGTGGCCGGTCGGTCGGTGGCGCT	105661	105684	ORF62	GGTCGTATGCAAGAGCAGGGTCCGAGGTATCCATCGCACGCATCGCACTGCATACGACCAGCGCCAC	TATATATATCGTGGCCGGTCGGTCG
VZVsncRNA16	GTGTTTGCATCGTCGCGCACCT	106124	106145	ORF62	GGTCGTATGCAAGAGCAGGGTCCGAGGTATCCATCGCACGCATCGCACTGCATACGACCAGGTGCGC	GTAGCGAGTGTTTGCATCGTC
VZVsncRNA17	ACTGTCGACCCGAGACCTGGCCTT	106354	106377	ORF62	GGTCGTATGCAAGAGCAGGGTCCGAGGTATCCATCGCACGCATCGCACTGCATACGACCAAGGCCAG	TATGATACTGTCGACCCGAGAC
VZVsncRNA18	AGACCCGGAGGATGTGAGGCTTCT	106597	106620	ORF62	GGTCGTATGCAAGAGCAGGGTCCGAGGTATCCATCGCACGCATCGCACTGCATACGACCAGAAGCCT	TATAGAGACCCGGAGGATGTG
VZVsncRNA19	GACGGACCGGCCCCAAACGGGGGA	106881	106904	ORF62	GGTCGTATGCAAGAGCAGGGTCCGAGGTATCCATCGCACGCATCGCACTGCATACGACCTCCCCCGT	TATATATAGACGGACCGGCCCCAA
VZVsncRNA20	AATGATTTCTGTCTCTGGCGCC	107803	107824	ORF62	GGTCGTATGCAAGAGCAGGGTCCGAGGTATCCATCGCACGCATCGCACTGCATACGACC GGCGCCAG	GCGGGCAATGATTTCTGTCT
VZVsncRNA21	CTTTTTACCCGAGATGGACTGAGT	108486	108509	ORF62	GGTCGTATGCAAGAGCAGGGTCCGAGGTATCCATCGCACGCATCGCACTGCATACGACCACTCAGTC	GCGCTACTTTTTACCCGAGATG
VZVsncRNA22	TTTGACGGCTGCGAGAGCGTT	109171	109191	ORF62-Promoter	GGTCGTATGCAAGAGCAGGGTCCGAGGTATCCATCGCACGCATCGCACTGCATACGACCAACGCTCT	AGTACCTTTGACGGCTGCG
VZVsncRNA23	TACGCCAATCGGATACACTCTTTT	110088	110111	ORF62-Promoter	GGTCGTATGCAAGAGCAGGGTCCGAGGTATCCATCGCACGCATCGCACTGCATACGACCAAAGAGTG	AGACGTACGCCAATCGGATA
VZVsncRNA24	ATTCAGATCATGCGGAGTCTTCA	115974	115996	ORF68	GGTCGTATGCAAGAGCAGGGTCCGAGGTATCCATCGCACGCATCGCACTGCATACGACCTGAAGACT	GCGTAGATTCAGATCATGCGG
miR26a		host			GGTCGTATGCAAGAGCAGGGTCCGAGGTATCCATCGCACGCATCGCACTGCATACGACCAGCCTATC	GCATGGCGTTCAAGTAATCCAG

Table 2
Detection of VZVsncRNA by stem-loop RT-qPCR in infected ARPE19 cells.

VZVsncRNA	qPCR + /n (%)	NGS reads
sncRNA 1	**2/4 (50%)**	18
sncRNA 2	**4/8 (50%)**	349
sncRNA 3	0/4 (0)	2
sncRNA 4	2/3 (67%)	0
sncRNA 5	**2/3 (67%)**	14
sncRNA 6	5/5 (100%)	22
sncRNA 7	**3/4 (75%)**	24
sncRNA 8	**1/3 (33%)**	17
sncRNA 9	**5/5 (100%)**	612
sncRNA 10	**4/4 (100%)**	12
sncRNA 11	3/3 (100%)	8
sncRNA 12	**3/3 (100%)**	15
sncRNA 13	5/5 (100%)	49
sncRNA 14	**4/5 (80%)**	29
sncRNA 15	**1/3 (33%)**	14
sncRNA 16	3/3 (100%)	6
sncRNA 17	**5/5 (100%)**	115
sncRNA 18	3/3 (100%)	9
sncRNA 19	2/3 (67%)	6
sncRNA 20	**1/5 (20%)**	30
sncRNA 21	1/2 (50%)	8
sncRNA 22	**1/7(14%)**	505
sncRNA 23	**3/6 (50%)**	108
sncRNA24	2/2 (100%)	14

The second column shows the number of experiments in which the difference between the signal from RNA extracted from mock infected and infected ARPE19 cells was at least 3 cycles (qPCR +)/the total number of independent experimental assays. The percentage of experiments where the VZVsncRNA was amplified as a percentage of the extractions assayed is in parenthesis for direct comparison. Values in **bold** are for those VZVsncRNA that were detected in the culture medium, as well as in the cytoplasm of infected cells. For comparison to results from our NGS analysis (Markus et al., 2017), counts for the VZVsncRNA detected in VZV-infected human fibroblasts are presented in the 3rd column.

3.2. Human neurons productively infected with VZV express 19 predicted VZVsncRNA

VZV genomes in neurons of the peripheral nervous system generate infectious virus after reactivation during herpes zoster that is transported anterogradely in axons to infect peripheral tissues. Our previous study detected NGS counts for all the predicted sequences of potential VZVsncRNA in productively infected neurons derived from hESC, but the presence of only one of these was confirmed using SL-PCR. To assay for the presence of the other VZVsncRNA by SL-PCR in infected human neurons, we generated neurons from hESC using two different methods. The first was that used in our NGS study, where neural differentiation of hESC was induced by co-culture with PA6 murine stromal cells ((Pomp et al., 2008), (Markus et al., 2017)). The second method used to generate neurons was induction of differentiation with growth factors (without the use of animal feeder cells) much as described previously (Birenboim et al., 2013, see methods). Micrographs of a living neuronal culture prepared with this second method and infected with VZV66GFP are shown in Fig. 1D–F, and micrographs of fixed neurons prepared with this method stained for neurofilament proteins are shown in Fig. 1G and H.

The small RNA fraction extracted from VZV-infected neurons generated by both methods contained 19 of the predicted VZVsncRNA by SL-PCR analysis (Table 3). VZVsncRNA3 was not detected in infected neurons in three separate experiments, as observed for infected ARPE19 cells. Importantly, all four VZVsncRNA mapping antisense to introns of the recently-described VZV latency associated transcript VLT (Depledge et al., 2018) VZVsncRNA10-VZVsncRNA13), were detected in productively infected neurons in most of the preparations. VZVsncRNA9, which was previously detected at the highest levels in neurons in our NGS data, was detected in the current study by SL-PCR in 75% of neuronal RNA preparations. There were differences between neurons

Table 3
Detection of VZVsncRNA by stem-loop RT-qPCR in infected hESC-derived neurons.

VZVsncRNA	qPCR + /n (%)	NGS counts
sncRNA 1	2/4 (50%)	6
sncRNA 2	0/3 (0)	26
sncRNA 3	0/3 (0)	28
sncRNA 4	3/3 (100%)	25
sncRNA 5	1/2 (50%)	12
sncRNA 6	2/3 (67%)	5
sncRNA 7	3/3 (100%)	7
sncRNA 8	1/4 (25%)	46
sncRNA 9	3/4 (75%)	126
sncRNA 10	2/3 (67%)	30
sncRNA 11	2/3 (67%)	18
sncRNA 12	3/3 (100%)	13
sncRNA 13	2/3 (67%)	24
sncRNA 14	3/3 (100%)	4
sncRNA 15	0/3 (0)	37
sncRNA 16	3/3 (100%)	19
sncRNA 17	3/4 (75%)	61
sncRNA 18	3/4 (75%)	32
sncRNA 19	0/2 (0)	24
sncRNA 20	3/4 (75%)	12
sncRNA 21	1/4 (25%)	50
sncRNA 22	0/5 (0)	1047
sncRNA 23	1/6 (16%)	15
sncRNA24	1/3 (33%)	21

The second column shows the number of experiments in which the difference between the signal from RNA extracted from mock infected and productively infected human embryonic stem cell-derived neurons was at least 3 cycles (qPCR +) as a proportion of the total number of independent experimental assays. The percentage of experiments where the VZVsncRNA was amplified as a percentage of the extractions assayed is given in parenthesis for direct comparison. For comparison to results from our NGS analysis (Markus et al., 2017), counts for the VZVsncRNA detected in VZV-infected neurons are presented in the 3rd column.

and ARPE19 cells in terms of frequency of detection of some VZVsncRNA. For example, VZVsncRNA20 was detected in three of four RNA extracts from neurons tested, but only in 1 of 5 extractions from ARPE19 cells. Again, the levels of NGS counts for VZVsncRNA in neurons did not necessarily correlate with levels detected by SL-PCR, as seen in ARPE19 cells. For example, while NGS counts for VZVsncRNA22 were highest in neurons, the VZVsncRNA was not detected by SL-PCR in any of five experiments. In contrast, VZVsncRNA1, VZVsncRNA6, VZVsncRNA7, and VZVsncRNA14, which all showed less than 10 NGS counts in our previous study, were detected by SL PCR in at least 75% of experiments. The reason for this disparity between detection with the two methods remains to be elucidated.

3.3. Different effects of blocking two VZVsncRNA on viral growth in ARPE19 cells

After confirming the presence of almost all the bioinformatically-predicted VZVsncRNA by SL-PCR, we examined whether some of these molecules may contribute to the regulation of VZV lytic replication. We selected two VZVsncRNA to test using a live cell-imaging assay after transfection of locked nucleic acid (LNA) antagonists to each VZVsncRNA (Markus et al., 2017). These were 1) VZVsncRNA2, detected in most (5/8) experiments by SL-PCR and 2) VZVsncRNA20, detected only in 1 of 5 extractions from both ARPE19 cells and neurons cells. Transfection of an LNA antagonist to VZVsncRNA2 did not result in a significant effect on spread of foci of infection of VZV infection (FOI) (n = 3, Fig. 2A–C). In contrast, transfection of an LNA antagonist to VZVsncRNA20 enhanced FOI growth, both on the average and in each experiment (n = 3, Fig. 2D and E). Observing fluorescent FOI allowed us to follow infection in living cultures daily, and the effects of the LNA antagonist were significant by this assay from 3d post-

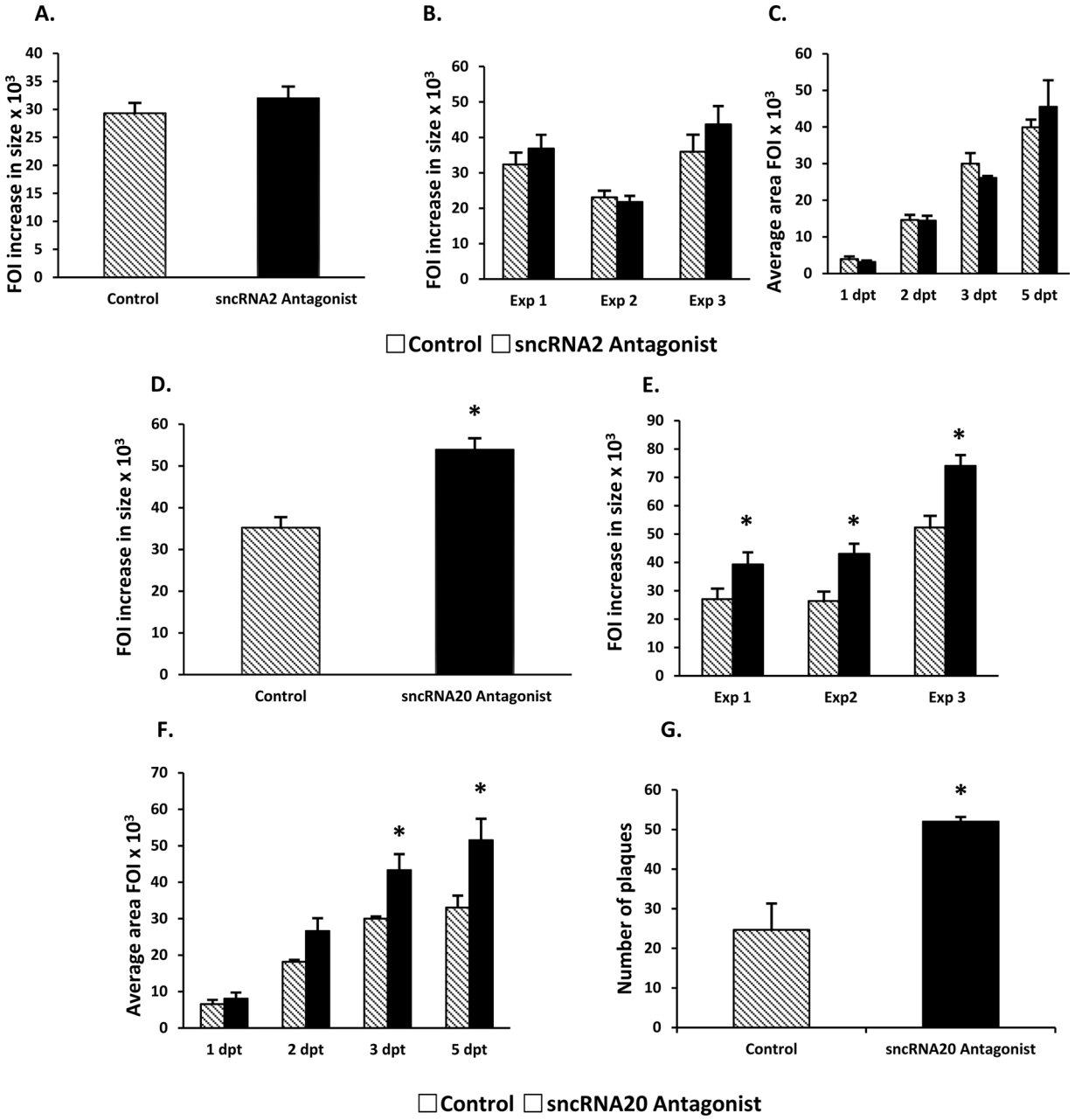

Fig. 2. Effect on growth of VZV infectious foci and the numbers of viral plaques after transfection of antagonists to two VZVsncRNA.
Locked antagonists to VZVsncRNA2 (A–C) or to VZVsncRNA20 (D–G) were transfected one day after seeding small numbers of VZVRFP66-infected ARPE19 cells onto monolayers of ARPE19. A scrambled sequence was transfected as a control. More than 80 FOI were measured for each experimental condition. The graphs in A and D show the average change in size of individual foci of infection (FOI) between 1dpi to 5dpi in pixel units. No difference in growth of FOI was seen between control and VZVsncRNA2 antagonist transfected wells (A, n = 3). When an antagonist to VZVsncRNA20 was transfected, it increased the growth of the FOI by an average of 50% (D, n = 3, $p < 0.02$). The data for the individual experiments presented as averages in A and D are shown in B and E respectively. RFP-expressing viruses allowed examination of the FOI continuously and revealed that the differences in FOI size were inconsistent at all time points for VZVsncRNA2 (C) and significantly different by 3 days after infection for VZVsncRNA20 (F). Cells from antagonist and scrambled RNA-transfected wells 7dpi were used to infect naïve ARPE19 cells, and standard plaque assays were performed. The transfection of the antagonist resulted in about twice as many infectious plaques as the control, scrambled RNA (G) (n = 2, data from one of two experiments with similar results). Asterisks indicate statistical significance between control and transfected wells ($p < 0.05$).

transfection of the inhibitor (Fig. 2F). FOI growth does not necessarily represent an increase in infectious virus, rather it measures the spread of the virus. In order to obtain a more direct measure of the effect of VZVsncRNA in the quantity of infectious virus generated, plaque assays were performed with cells from two of the three experiments with the LNA antagonist to VZVsncRNA20. In both experiments there was a significant increase in the number of plaques formed by cells from the wells treated with the inhibitor: in one experiment the inhibitor transfection resulted in a 100% increase in plaques (25 ± 6 in the control versus 52 ± 1 plaques in the inhibitor treated, $p < 0.02$) and a 50% increase in the other experiment (23 ± 1 control, 34 ± 2 inhibitor, $p < 0.01$). These results, together with our previous observation that an LNA antagonist to VZVsncRNA23 increases VZV replication, indicate that some but perhaps not all SL-PCR detected VZVsncRNA may regulate VZV replication in culture.

4. Discussion

In the present study, we used Taqman SL-PCR to probe small RNA from VZV-infected ARPE19 cells and found that 23 of 24 sequences previously predicted to be small RNA species encoded by VZV were indeed detected. This indicates that the novel prediction method used to evaluate NGS reads of small RNA, manual alignment of similar sequences, is indeed a viable predictive approach (Markus et al., 2017). The current findings suggest that VZV is like other herpesviruses and expresses multiple small RNAs in lytic infection. We have not yet been able to precipitate these VZVsncRNA with antibodies to AGO2, and, except for VZVsncRNA23, they are not predicted to fold as miR. The VZVsncRNA species we have identified therefore may not be miR, and their biogenesis, characteristics and mechanisms of action remain to be elucidated.

A great deal of variability was observed both within and between experiments in terms of the detection of the VZVsncRNA. Some were only detected once by SL-PCR in several RNA preparations, while others were detected in every RNA preparation. Similarly, the levels of the VZVsncRNA detected varied greatly (Supplementary Table 1). Since each stem-loop PCR reaction requires a separate RT reaction, large amounts of RNA are required for these assays it is very difficult to test for all sncRNA from a single RNA extraction. The variability in levels and frequency of detection of the VZVsncRNA that we encountered could be due to several factors. It is possible that these small RNAs are broken down rapidly, or that variability arises from differences in cell-lysis from infection, and/or the extractions themselves since they were performed by several different investigators could have yielded different amounts of the VZVsncRNA in different experiments. In addition, VZV infection of ARPE19 cells was performed by cell-associated infection which is not synchronous. This results in heterogeneity in the stages of the viral replications cycle in different experiments, which also probably contributed to the variation in VZVsncRNA detection from sample to sample. Because of this issue of variability, we assayed for some of the VZVsncRNA many times (Table 2), particularly those that were encoded by genomic regions of interest or were present at high count number in our NGS data.

There is accumulating evidence that small non-coding RNAs, especially miR, are secreted and may exert their effects on other cells after being transported in small membrane-deliminated vesicles such as exosomes (i.e. Kalamvoki et al., 2014). In preliminary experiments we detected the presence of many of the VZV sncRNA in the medium using two protocols for isolating and concentrating exosomes, and this fraction was immunopositive for the exosomal marker CD81 (not shown). However, since exosomes and VZV virions are similar in size, we cannot be sure that the VZVsncRNA we detected in this fraction was in exosomes or in viral particles or both. The secretion of alphaherpesvirus miR ((Kalamvoki et al., 2014),(Han et al., 2016)) suggests that further investigation into the export of VZVsncRNA may be worthwhile.

We previously showed that VZVsncRNA23 represses spread of VZV, since the transfection of an LNA antagonist to it resulted in a significant increase in FOI size using a live-imaging assay (Markus et al., 2017). That initial study was expanded here by assaying antagonists to two additional VZVsncRNA for their effects on the spread of VZV. The antagonist to VZVsncRNA20 increased the spread of FOI, while that to VZVsncRNA2 did not have a significant effect. FOI measurements using fluorescent indicator viruses only report cells expressing the VZV-fluorescent fusion protein. Plaque assays complemented these experiments and indicated that the larger FOI from wells treated with the antagonist to VZVsncRNA20 included larger numbers of VZV-infected cells capable of infecting naïve cells. These results suggest that VZVsncRNA20 is a biologically relevant molecule in the replication of VZV and acts to repress productive infection. Similar results were reported for two HSV miRNA, miR-H28 and miR-H29 (Han et al., 2016).

The VZVsncRNA2 antagonist, despite this VZVsncRNA often being detected by SL-PCR and being present at relatively high levels in the NGS study, lacked a modulating effect on VZV spread. A possible explanation is that multiple transcripts containing this coding sequence of this sncRNA have been recently described (Prazsák et al., 2018). Its sequence is included in a monocistronic form of ORF10, a bicistronic form ORF 9–10 and a tricistronic form ORF9A-9–10 and it may be generated from all of them without having an actual physiological role. Such RNAs would still be detected by SL-PCR or as NGS counts. Other possibilities include the timing of the transfection, the concentration of the antagonist, the sensitivity of the assay, or an effect on some aspect of the viral life cycle not easily observed in these cells. Study of additional VZV-permissive cell types may reveal that they function in a cell-type specific role. Our results obtained from inhibition of VZVsncRNA20 indicate that the reverse is also true regarding NGS counts and function: the presence of a sequence at low levels in NGS does not eliminate the possibility that the sncRNA can play a role in the life-cycle of the virus.

Two of the VZVsncRNA detected by both NGS (Markus et al., 2017) and by the SL- PCR assay used here are VZVsncRNA12 and VZVsncRNA13. Both are encoded within the apparent leader sequence of ORF61 and are antisense to introns of the recently reported spliced latency-associated transcript, VLT. The VLT transcript was detected not only in human post-mortem latent infected ganglia, but also in productively infected cells (Depledge et al., 2018). It is therefore important to determine if these VZVsncRNA can modulate lytic and latent infections. Studies inhibiting these VZVsncRNA in lytically-infected ARPE19 cultures using LNA antagonists are ongoing. However, due to the small numbers of latently-infected neurons obtained in our cultures the SL-PCR assay may not be sensitive enough to detect VZVsncRNA in them. Future improvements in the efficiency of establishment of latency in our in-vitro system may reveal if these VZVsncRNA are expressed during VZV latency and if they influence productive or latent infections in neurons, as seen in for miR in other herpesviruses.

The field of therapeutics based on short oligonucleotides and targeting RNA (reviewed recently in (Crooke et al., 2018; Levin, 2019) including targeting miR (Simonson and Das, 2015), has seen an explosion in the past several years. Since we have now found that at least two of the VZVsncRNA are able to modulate VZV growth in culture, study of VZVsncRNA may not only provide new insights into the biology of VZV infection, but also inform the development of novel therapeutics for VZV infection, especially painful herpes zoster.

Acknowledgements

This research was supported by NIH grant R01 AI122640 and US-Israel Binational Science Foundation2017259 to RG and PRK. RG was also supported by Israel Science Foundation grant 254/16. PRK acknowledges additional support from core grant EY08098, and unrestricted funds from Research to Prevent Blindness, Inc and The Eye & Ear foundation of Pittsburgh. Linoy Golani was supported in part by a President's PhD fellowship from Bar-Ilan University. Thanks to Dr. Amos Markus for many helpful discussions and critical reading of the manuscript, and to Dr. Moran Topf for technical assistance. Monoclonal antibody was developed by Drs. M. McCutcheon and S. Carroll was obtained from the Developmental Studies Hybridoma Bank developed under the auspices of the NICHD and maintained by The University of Iowa.

Appendix A. Supplementary data

Supplementary material related to this article can be found, in the online version, at doi:https://doi.org/10.1016/j.virusres.2019.197773.

References

Birenboim, R., Markus, A., Goldstein, R.S., 2013. Simple generation of neurons from human embryonic stem cells using agarose multiwell dishes. J. Neurosci. Methods

214, 9–14. https://doi.org/10.1016/j.jneumeth.2012.12.026.
Crooke, S.T., Witztum, J.L., Bennett, C.F., Baker, B.F., 2018. RNA-targeted therapeutics. Cell Metab. 27, 714–739. https://doi.org/10.1016/j.cmet.2018.03.004.
Cullen, B.R., 2011. Herpesvirus microRNAs: phenotypes and functions. Curr. Opin. Virol. 1, 211–215. https://doi.org/10.1016/j.coviro.2011.04.003.
Depledge, D.P., Ouwendijk, W.J.D., Sadaoka, T., Braspenning, S.E., Mori, Y., Cohrs, R.J., Verjans, G.M.G.M., Breuer, J., 2018. A spliced latency-associated VZV transcript maps antisense to the viral transactivator gene 61. Nat. Commun. 9, 1167. https://doi.org/10.1038/s41467-018-03569-2.
Erazo, A., Yee, M.B., Osterrieder, N., Kinchington, P.R., 2008. Varicella-zoster virus open reading frame 66 protein kinase is required for efficient viral growth in primary human corneal stromal fibroblast cells. J. Virol. 82, 7653–7665. https://doi.org/10.1128/JVI.00311-08.
Han, Z., Liu, X., Chen, X., Zhou, X., Du, T., Roizman, B., Zhou, G., 2016. miR-H28 and miR-H29 expressed late in productive infection are exported and restrict HSV-1 replication and spread in recipient cells. Proc. Natl. Acad. Sci. 113, E894–E901. https://doi.org/10.1073/pnas.1525674113.
Kalamvoki, M., Du, T., Roizman, B., 2014. Cells infected with herpes simplex virus 1 export to uninfected cells exosomes containing STING, viral mRNAs, and microRNAs. Proc. Natl. Acad. Sci. 111, E4991–E4996. https://doi.org/10.1073/pnas.1419338111.
Kawasaki, H., Mizuseki, K., Nishikawa, S., Kaneko, S., Kuwana, Y., Nakanishi, S., Nishikawa, S.-I., Sasai, Y., 2000. Induction of midbrain dopaminergic neurons from ES cells by stromal cell-derived activity. Neuron 28, 31–40.
Levin, A.A., 2019. Treating disease at the RNA level with oligonucleotides. N. Engl. J. Med. 380, 57–70. https://doi.org/10.1056/NEJMra1705346.
Markus, A., Golani, L., Ojha, N.K., Borodiansky-Shteinberg, T., Kinchington, P.R., Goldstein, R.S., 2017. Varicella zoster virus expresses multiple small non-coding RNAs. J. Virol. https://doi.org/10.1128/JVI.01710-17. JVI.01710-17.
Mohammadi-Yeganeh, S., Paryan, M., Mirab Samiee, S., Soleimani, M., Arefian, E., Azadmanesh, K., Mostafavi, E., Mahdian, R., Karimipoor, M., 2013. Development of a robust, low cost stem-loop real-time quantification PCR technique for miRNA expression analysis. Mol. Biol. Rep. 40, 3665–3674. https://doi.org/10.1007/s11033-012-2442-x.
Piedade, D., Azevedo-Pereira, J.M., 2016. The role of microRNAs in the pathogenesis of herpesvirus infection. Viruses 8. https://doi.org/10.3390/v8060156.
Pomp, O., Brokhman, I., Ben-Dor, I., Reubinoff, B., Goldstein, R.S., 2005. Generation of peripheral sensory and sympathetic neurons and neural crest cells from human embryonic stem cells. Stem Cells 23, 923–930.
Pomp, O., Brokhman, I., Ziegler, L., Almog, M., Korngreen, A., Tavian, M., Goldstein, R.S., 2008. PA6-induced human embryonic stem cell-derived neurospheres: a new source of human peripheral sensory neurons and neural crest cells. Brain Res. 1230, 50–60.
Prazsák, I., Moldován, N., Balázs, Z., Tombácz, D., Megyeri, K., Szűcs, A., Csabai, Z., Boldogkői, Z., 2018. Long-read sequencing uncovers a complex transcriptome topology in varicella zoster virus. BMC Genomics 19, 873. https://doi.org/10.1186/s12864-018-5267-8.
Simonson, B., Das, S., 2015. MicroRNA therapeutics: the next magic bullet? Mini Rev. Med. Chem. 15, 467–474.
Sloutskin, A., Goldstein, R.S., 2014. Laboratory preparation of Varicella-zoster virus: concentration of virus-containing supernatant, use of a debris fraction and magnetofection for consistent cell-free VZV infections. J. Virol. Methods 206, 128–132. https://doi.org/10.1016/j.jviromet.2014.05.027.
Tischer, B.K., Kaufer, B.B., Sommer, M., Wussow, F., Arvin, A.M., Osterrieder, N., 2007. A self-excisable infectious bacterial artificial chromosome clone of varicella-zoster virus allows analysis of the essential tegument protein encoded by ORF9. J. Virol. 81, 13200–13208. https://doi.org/10.1128/JVI.01148-07.
Umbach, J.L., Nagel, M.A., Cohrs, R.J., Gilden, D.H., Cullen, B.R., 2009. Analysis of human alphaherpesvirus microRNA expression in latently infected human trigeminal ganglia. J. Virol. 83, 10677–10683. https://doi.org/10.1128/JVI.01185-09.
Watson, S., Mercier, S., Bye, C., Wilkinson, J., Cunningham, A.L., Harman, A.N., 2007. Determination of suitable housekeeping genes for normalisation of quantitative real time PCR analysis of cells infected with human immunodeficiency virus and herpes viruses. Virol. J. 4, 130. https://doi.org/10.1186/1743-422X-4-130.